From Materials to Structures: Advancement through Innovation – Samali, Attard & Song (Eds)
© 2013 Taylor & Francis Group, London, ISBN 978-0-415-63318-5

Investigation into cavitation as a cause of rate-dependent fatigue loss in submerged concrete members

M. Sagan, C. Fujiyama & K. Maekawa
Department of Civil Engineering, School of Engineering, The University of Tokyo, Japan

ABSTRACT: Water is known to decrease the fatigue life of concrete members. The reduction can be partially explained by the established water-induced reductions in both shear transfer and compressive strength, but even considering these two phenomena, there is still an order of magnitude that is unaccounted for. The authors investigated the effect of loading rate-dependent pore pressure changes on fatigue life. Rate-dependence has been observed, but results also predict low pore pressures. Such pressures may lead to cavitation in concrete cracks, which may be a significant factor in loss of fatigue life. The authors attempted to verify the presence of cavitation both visually and through sonic pressure data. Experiments were performed on concrete members using various different loading conditions to induce rapid crack opening and closing. Research into this topic may prove to be beneficial in the prediction of cavitation, and ultimately to develop a relationship between dynamic loading conditions and loss of fatigue strength through cavitation.

1 INTRODUCTION

The reduction of compressive strength in submerged concrete has been well-documented in both experiment and practice, and many design codes already have clauses that give a simple reduction factor. Similarly, the loss of shear transfer due to water is also known, and empirical models providing a reduction factor based on crack shear and opening displacement exist (Maekawa et al. 2006).

The reduction of fatigue strength in submerged concrete has also been documented in recent years. This is of particular relevance to bridge decks subjected to high cycles of traffic and exposed to the environment, where it is a major source of damage.

Until the late 70's, fatigue strength (the stress level that a member could undergo before failure at 2,000,000 cycles) of concrete was thought to be 55–60% of static strength, regardless of environmental conditions. However, subsequent research found that the fatigue strength in water was reduced to 30% of the static strength in water (Ozaki & Shimura 1980). Sources have since reported that the reduction in fatigue life (number of cycles until failure) under submerged conditions is 1/200 (Matsui 1987). While the mechanism has not been qualitatively explained, it is reasonable to believe that it is partially attributable to both compressive strength loss and shear transfer loss described above. However, even coupling these losses (Fig. 1), there is still an order of magnitude separating the difference predicted in analysis and the difference observed in experiment (Fig. 2). Note that this study is restricted to standard temperatures, so the influence of water discussed in this paper excludes the well-known phenomena of freeze-thaw action.

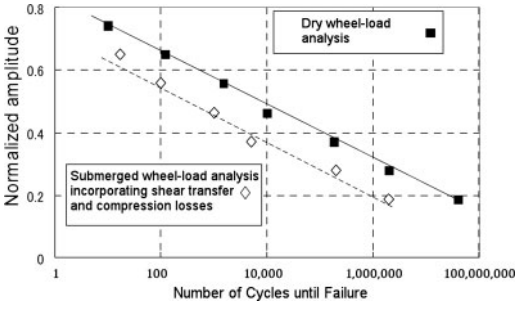

Figure 1. Analytical S-N diagram showing fatigue life of RC slabs undergoing wheel-type loading, including reductions for Shear Transfer and Compression. An order of magnitude different from observed results (Maekawa et al. 2006). Note that an S-N ("Stress-Number of cycles") diagram gives the number of cycles that a member can be subjected to before failure, where the maximum stress in each cycle is a certain fraction of its static strength (this fraction is the normalized amplitude).

In addition to the general unexplained loss of fatigue life in the presence of water, there seems to be a strong rate-dependency, wherein rapidly-applied loads will cause failure under significantly fewer cycles than slowly-applied loads. This trend will be analyzed and qualitative explanations will be suggested.

2 MODELLING

2.1 *Modelling of concrete and water*

It is reasonable to assume that one of the chief parameters contributing to the water-induced reduction of

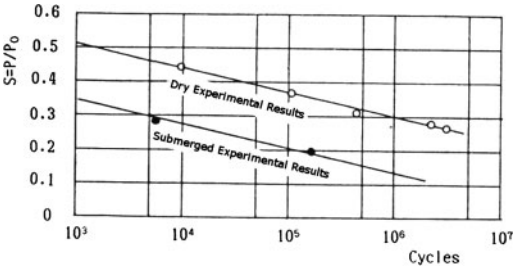

Figure 2. Experimental S-N diagram showing fatigue life of RC slabs. The submerged case had a fatigue life 1/200 that of dry case (Matsui 1987).

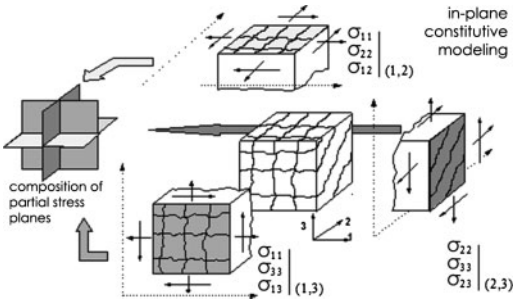

Figure 3. COM3 system used for nonlinear analysis of reinforced concrete. Fundamental constitutive relations exist for compression, tension and shear transfer.

concrete fatigue life is the pore-water pressure. While moisture within concrete pores can travel relatively freely over long periods of time, water's viscosity may stifle the movement under rapid deformation in the concrete skeleton. If water (generally considered to be an "incompressible fluid") is unable to move freely, even small deformation of the concrete skeleton would cause sharp rises or falls in pore-pressure. These pressures exerted on the concrete skeleton could cause accelerated damage and reduced fatigue life. If pore-pressure is indeed a key parameter in this study, then the reduction of concrete fatigue life should have a significant loading rate-dependency.

It was deemed necessary to have a model that deals with moisture kinematics from the concrete skeleton. Biot's theory for porous materials (Biot 1941), commonly used in fields such as geotechnical engineering, was utilized to model concrete as a two-phase system.

The theory was implemented on top of COM3 (Fig. 3), a nonlinear analysis method for modelling reinforced concrete in three dimensions using constitutive relations, supporting multi-directional cracking and progressive damage.

2.2 *Implementation of Biot's model*

Biot's model assumes stress in the structure is influenced isotropically by pore-water pressure, i.e.:

$$\sigma_{ij} = \sigma^*_{ij} + \delta_{ij} \cdot p \tag{1}$$

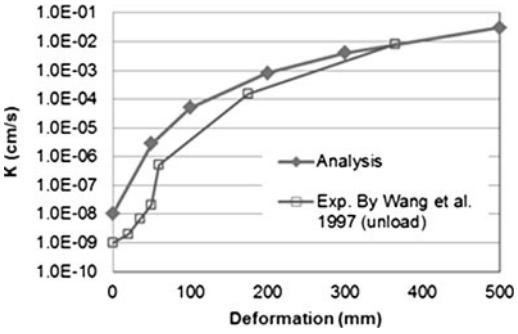

Figure 4. Permeability-deformation relationship to be used in analysis based on empirical data (Wang et al. 1997).

where σ_{ij} is total stress, σ^*_{ij} is the effective stress on the solid skeleton, δ_{ij} is the unit tensor, and p is the scalar pore-water pressure. This assumption does not apply in the situation we are interested in, namely the stress on crack surfaces, which are anisotropic based on the stress history. Clearly, pore-water pressure will act perpendicular to the crack. Thus we have updated the model with:

$$\sigma_{ij} = \sigma^*_{ij} + \delta_{ij} \cdot l_i \cdot p \tag{2}$$

where l_i is the unit directional vector normal to the crack plane.

Taking u as the displacement of the skeleton, w as the displacement of pore-water, n as the porosity and κ as permeability, the dynamic equilibrium of phases can be written as:

$$\sigma_{ij,j} = \rho(\ddot{u}_i - g_i) + \rho_w \ddot{w}_i \tag{3}$$

$$p_{,i} = \rho_w(\ddot{u}_i - g_i) + \rho_w \ddot{w}_i / n + {}^{1}\!/_{\kappa_i}\, \dot{w}_i \tag{4}$$

where g is acceleration due to gravity and ρ and ρ_w are the densities of the concrete (including pores) and water respectively.

Utilizing studies of the relationship between permeability of cracked concrete and crack-opening displacement (Wang et al. 1997) (Fig. 4), a three-dimensional relationship was developed giving the directional permeability κ_i as a function of the transverse strains ε_{jj} and ε_{kk}:

$$\kappa_i = \kappa^* \left\{ 1 + \left(\frac{\varepsilon_{jj} + \varepsilon_{kk}}{a} \right)^4 \right\} \tag{5}$$

where κ^* is the intrinsic permeability and a is determined through experiment.

As negative pressures in the original Biot formulation were unrestricted, an updated relation was developed, restricting negative pressures to a vacuum using the following relation (with the convention being that $p = 1$ atm represents a vacuum, $p = 0$ represents

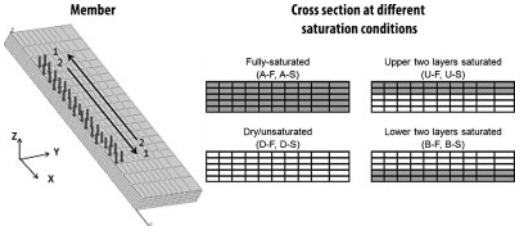

Figure 5. Mesh of deck member used in analysis. To reduce required processing, only one side of the deck member is modeled (taking advantage of symmetry).

atmospheric pressure, and $p < 0$ represents positive pressure):

$$w_{i,i} + \varepsilon_{ii} < 0 \longrightarrow p = K_f\left(w_{i,i} + \varepsilon_{ii}\right) \tag{6}$$

(compression, positive pressure)

$$w_{i,i} + \varepsilon_{ii} > 0 \longrightarrow p = \tanh\left\{K_f\left(w_{i,i} + \varepsilon_{ii}\right)\right\} \tag{7}$$

(tension, negative pressure)

$$K_f = \left(\frac{1-n}{K_c} + \frac{n}{K_w}\right)^{-1} \tag{8}$$

where K_w, K_c and K_f are the bulk moduli of water, the concrete skeleton and composite respectively.

2.3 *Analysis*

Computational analysis was performed on a deck member of dimensions L3000 × W2000 × D190 mm, the same as what was used in a related study (Matsui 1987) (Fig. 5). Only half the deck was modeled to take advantage of symmetry. A moving 80 kN wheel-load was simulated, travelling longitudinally along the top side of the member. Four different saturation scenarios were chosen: fully saturated, upper-side-saturated, lower-side-saturated, and dry. To determine the level of loading rate-dependence, different velocities of the wheel-load were used: 77 km/h and 0.77 km/h. With these four saturation cases and two speed cases, eight different cases (labeled for convenience in Table 1) were analysed.

Each case was processed, and the midspan displacement was extracted. The effect of the two wheel-load velocities was compared in each saturation case. (Note that for the following cases, although each cycle was individually processed, the graphs show a reduced number of oscillations at later stages for the sake of visual clarity.)

As expected, the difference between results in the dry case (D-F, D-S) was found to be almost negligible, suggesting that the fatigue life of concrete in dry conditions is loading rate-independent. Surprisingly, the lower-layer saturated case (B-F, B-S) also displayed very little rate-dependence, and the fatigue life was similar to that of the dry case. Possible reasons for this will be discussed shortly.

Table 1. Reference names of loading cases.

Loading Speed (km/h)	Saturation condition: Fully saturated	Upper two layers saturated	Lower two layers saturated	Dry
77.0	A-F	U-F	B-F	D-F
0.77	A-S	U-S	B-S	D-S

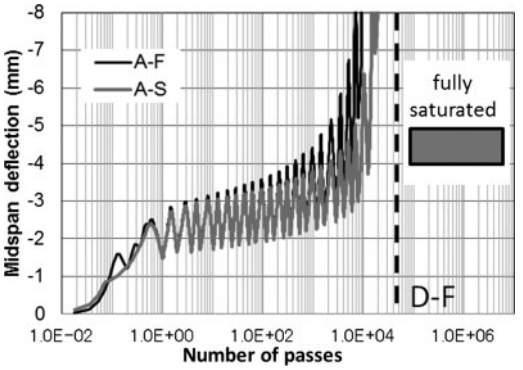

Figure 6. Analytical midspan deflection of RC deck member, fully saturated, under wheel-type loading at 77 km/h (A-F) and 0.77 km/h (A-S).

The fully-saturated case (A-F, A-S) showed a lower fatigue life than the previous cases, and also showed some rate-dependence, with the fatigue life under the fast loading rate was about 1/2 to 1/3 that of the slow-case (Fig. 6). Perhaps most interestingly, the upper-layer saturated case (U-F, U-S) showed a high level of rate-dependence. While the slower loading rate (U-S) gave a longer fatigue than the fully-saturated case (both A-F and A-S), the faster loading rate (U-F) had a lower fatigue life than the fully-saturated case, about 1/8 that of the slow-case (Fig. 7).

The reason why the analysis shows that upper-side-saturated case seems to be more rate-dependent is that restrictions on pore pressure have been imposed. The upper side of the bridge deck mainly undergoes compression, and positive pressure (compression) is unrestricted, allowing high pore pressures to be generated when under rapid deformation (Fig. 8), damaging the concrete skeleton. On the other hand, negative pressure (tension) is restricted, so the lower-side-saturated case which is mainly under tension does not experience high pore pressures (Fig. 9). (Note that negative pressures are denoted as positive numbers here, due to the tension-compression convention.)

One distinct difference between the rapid wheel-load and the slow wheel-load to note from Figure 9 is that the rapid case is reaching negative pressures that approach −1 atm (the vacuum pressure).

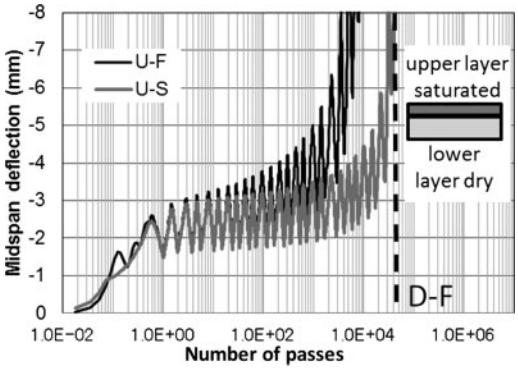

Figure 7. Analytical midspan deflection of RC deck member, with upper layer saturated, under wheel-type loading at 77 km/h (U-F) and 0.77 km/h (U-S).

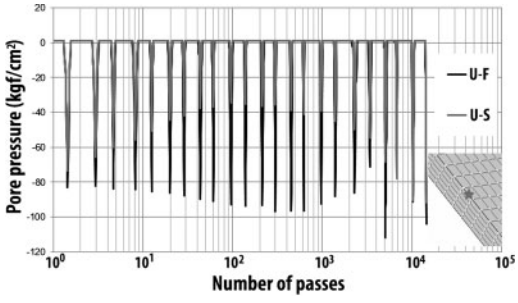

Figure 8. Pore pressure of upper element at midspan of RC deck, upper-layer-saturated, both fast and slow loading. High pressures responsible for apparent rate-dependent fatigue loss.

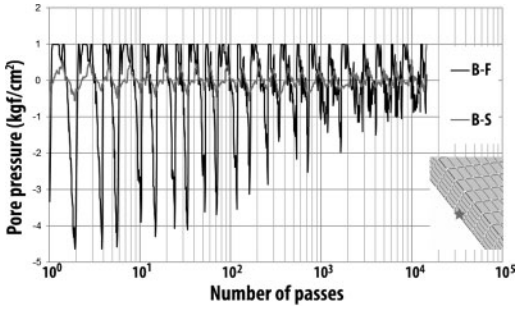

Figure 9. Pore pressure of lower element at midspan of RC deck, lower-layer-saturated, both fast and slow loading. Low pressures responsible for apparent lack of rate-dependency in fatigue loss.

The implications of this will be discussed in the next section.

3 CAVITATION

3.1 *Possible presence of cavitation*

Based on the above analysis, rapid loading of saturated concrete causes high pore-pressure changes, and of particular interest, "negative pressures" that approach −1 atm (or an absolute pressure of zero). According to basic physical chemistry, water with pressure reaching these values should vaporize (Fig. 10). This vapor should occur in the form of cavitation bubbles, which collapse soon after formation. The collapse produces a high-energy high-temperature jet (Fig. 11), which can damage materials that it comes into contact with. For this reason, cavitation is a leading cause of damage in high-cycle marine devices such as pumps and propellers (Fig. 10). If cavitation is present and causes comparable damage in submerged concrete under high-cycle loading, this phenomenon may be the cause of fatigue loss that can explain the difference between experiment and analysis that has existed up to this point.

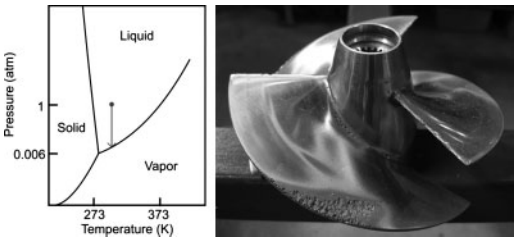

Figure 10. Left: Simple phase diagram of water, showing the occurrence of vaporization at low pressures. Right: A propeller that has experienced cavitation damage (Xahlee.org, 2003).

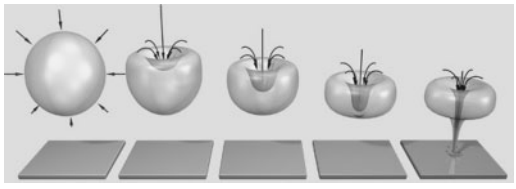

Figure 11. The process of cavitation damage on a surface. The progressive implosion of cavitation bubbles and formation of high-energy jets are displayed (Lockstockaue.com, 2012).

3.2 *Detection of cavitation*

To determine whether the predicted pressure drops indeed cause cavitation within the cracks of the concrete, experiments were performed. First, the issue of how to reliably detect the presence of cavitation was investigated. The method adopted was the analysis of sonic pressure data from the area of interest, in the hopes that the high frequency sound caused by bubble formation and collapse would be detectable by a hydrophone with a high sampling rate. Tests were performed on a submerged concrete column subjected to reverse-cycle push-over loading (Fig. 12), as well as simply-supported two beams subject to cyclic loading applied at midspan (Fig. 12), one concrete and one made from sheets of plexiglass (so that the crack area could be observed visually). Both had

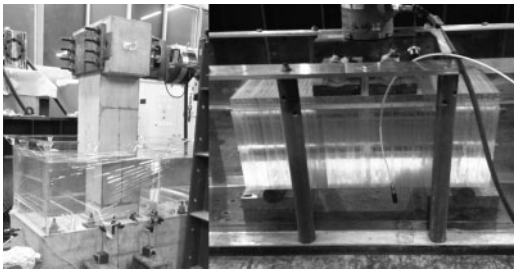

Figure 12. Left: Reverse-cyclic pushover test setup. Lower section submerged in water. Hydrophone is adjacent to base section. Right: Plexiglass specimen setup. Mostly submerged in water. Hydrophone is placed below midpoint.

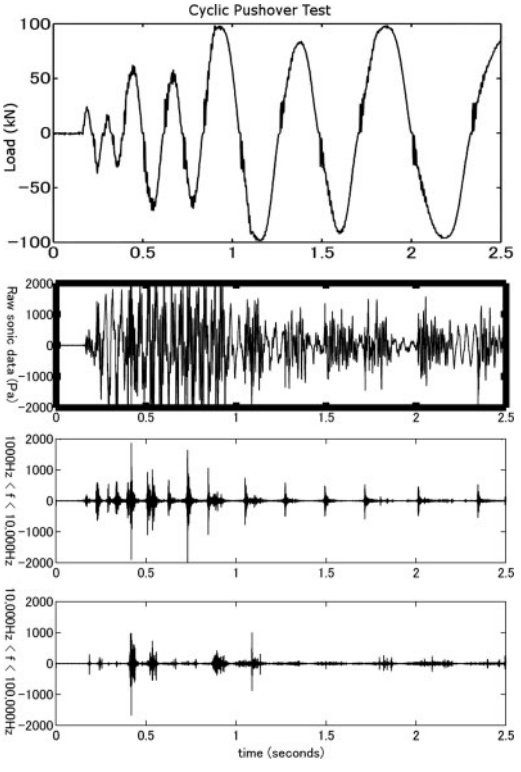

Figure 13. Loading data alongside hydrophone sonic data for reverse-cycle pushover test. The sonic data has been filtered into high frequency components. Some high-frequency sounds are observed during crack opening.

prefabricated cracks at midspan. The hydrophone was located directly adjacent to the specimen in each case.

The data recorded was sampled at 200 kHz, giving a Nyquist frequency (the highest detectable frequency for a given sampling rate) of 100 kHz.

3.3 *Interpretation of results*

The sonic data was analyzed using Fourier analysis, by both taking Short-Time Fourier Transforms (spectrograms) (Fig. 13) and filtering the signal into

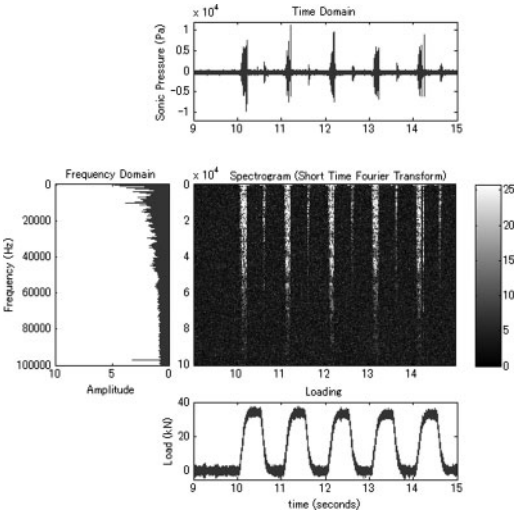

Figure 14. Submerged simply-supported plexiglass beam undergoing cyclic loading. Spectrogram of sonic data is shown with time-domain, frequency domain, and load data plotted alongside. The graphs indicate high pressures at high frequencies at crack-opening (coincident with loading) and lower pressures at lower frequencies at crack-closing (coincident with unloading).

different frequency components (Fig. 14). Under a variety of loading conditions, both methods tended to show higher frequency terms at crack opening stage.

This method became problematic when it was found that the sound of the specimen cracking caused the same high frequency periodic sounds that it had been hoped would be characteristic of cavitation, so it was decided that this method was insufficient. Additionally, the test conditions were such that water could travel freely into and out of the crack on opening and closing. This is not necessarily characteristic of the conditions of a bridge-deck, where cracks may be more isolated from free-flowing water.

Ultimately, testing has thus far yielded inconclusive results. Inherent flaws in the test design must be considered. Considering Figure 15, it is possible that the cavitation bubbles produced fall into the upper-left portion of the graph, those that are too small to be visible to the naked eye and have frequencies too high to be detected by the hydrophone used.

4 CONCLUSION

In light of the analysis presented in this paper, it is reasonable to assume that pore water pressure, which has shown to be highly rate-dependent, exerts non-negligible stresses on the concrete skeleton, causing damage. From this, we can say that pore water pressure is one of the chief parameters contributing to the water-induced reduction of concrete fatigue. The analyzed examples included a case in which a RC deck member was saturated only in the upper compressive layer, and

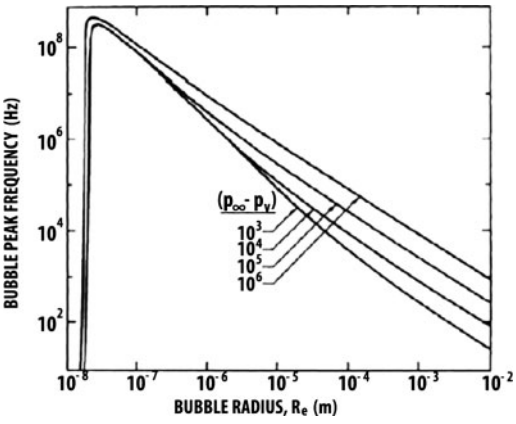

Figure 15. Cavitation bubble peak frequencies for corresponding bubble sizes. p_∞ and p_v denote reference pressure and vapor pressure respectively (Brennen 2011).

the rate-dependence of the fatigue life was almost an order of magnitude.

It has also been shown that, depending on the loading rate, pore pressures may reach that of vaporization, leading to the possibility of the occurrence of cavitation, which is a major cause of damage in high-cycle marine devices. Although the experiments performed so far have been unable to confirm this hypothesis, further studies will be undertaken.

It is possible that with the inclusion of losses due to rate-dependent cavitation damage and pore-pressures exerted on the concrete skeleton, an updated analytical model of water-induced fatigue loss (which currently includes water-induced compression and shear transfer losses) may be able to match the losses observed in experiment.

REFERENCES

Biot, M. A. 1941, General theory of three-dimensional consolidation, *Journal of Applied Physics*, 12, 155–164.

Brennen, C.E. 2011. Invited Lecture: An Introduction to Cavitation Fundamentals, *Warwick Innovative Manufacturing Research Forum 2011*.

Maekawa, K., Gebreyouhannes, E., Mishima, T. & An, X. 2006. Three-Dimensional Fatigue Simulation of RC Slabs under Traveling Wheel-Type Loads, *Journal of Advanced Concrete Technology*, Vol. 4, No. 3, 445–457.

Matsui, S. 1987. The Effect of Water on the Fatigue Strength of RC. Slabs Under Moving Loads, *Concrete Engineering Annual Report Compilation*, 9–2, pp. 627–632.

Ozaki, S. & Shimura, M. 1980. Compressive Fatigue Strength of Concrete in Water, *Proc. of the 35th Annual Conference of the Japan Society of Civil Engineers*, Vol. 5, pp. 293–294.

Ozaki, S., Sugata, N. & Mukaida, K. 1995. Investigation on the Reduction of Fatigue Strength of Submerged Concrete, *Proc. of International Conference on Concrete Under Service Conditions, CONSEC 2, 1694–1703*.

Wang, K., Jansen, D.C., Shah, S.P. & Karr, A.F. 1997. Permeability study of cracked concrete, *Cement and Concrete Research*, Volume 27, Issue 3.